

A Biodegradable Composite of Poly (3-hydroxybutyrate-co-3-hydroxyvalerate) (PHBV) with Short Cellulose Fiber for Packaging

Marceli N. Conceição^{a,b}, Mônica C.C. dos Santos^b, Javier M.A. Mancipe^c, Patricia S.C. Pereira^b,
Roberto C.C. Ribeiro^a, Rossana M.S.M. Thiré^c , Daniele C. Bastos^{b,*} 

^aCentro de Tecnologia Mineral, 21941-908, Rio de Janeiro, RJ, Brasil.

^bUniversidade do Estado do Rio de Janeiro, 23070-200, Rio de Janeiro, RJ, Brasil.

^cUniversidade Federal do Rio de Janeiro, 21941-599, Rio de Janeiro, RJ, Brasil.

Received: December 22, 2022; Revised: May 15, 2023; Accepted: May 25, 2023

The problem of improper disposal of polymeric waste is increasingly in present. Thus, the use of biodegradable polymers is a good alternative, especially for packaging. Compostable and biodegradable polymers such as PHBV can be completely degraded, making them ideal. But the short processability window and fluid instability is an important drawback to the wider application of this polymer in pure form. Production of composite materials has been indicated as a possibility for using this polymer. One source of filler is cellulose, because besides being widely available from agroindustrial waste. In this context, the present work reports the formulation of rigid packaging with PHBV and cellulose waste. An analytical mill was used to promote the dispersion of cellulose fibers. In general, the cellulose fibers increased the Vicat softening point of the polymeric matrix. There were more crystalline structures, according to DSC, and a decrease in impact strength, probably due to increased crystallinity and agglomerate formation. The microscopic analysis indicated greater surface roughness of the composite due to the increase of fibers, resulting in increased contact angle.

Keywords: PHBV, biodegradable composite, packaging.

1. Introduction

Because of the global growth in plastic use and poor plastic waste management, most plastic wastes end up on the earth's surface, followed by marine and fresh water bodies. Over long-time scales, plastics degrade into particles with sizes smaller than 5 mm, known as microplastics¹ that cause a much greater problem in microbiology or plants than can be observed^{2,3}.

Thus, the replacement with biodegradable polymers is a good alternative to mitigate this problem, especially for articles whose period of use and disposal is short, mainly those that are discarded after a single use, such as packaging, which accounts for the majority of polymeric waste. Some biopolymers are already used on an industrial scale, such as PLA, but despite their biodegradability, they are only compostable in an industrial environment and thus can still generate polymeric waste. In this context, poly (3-hydroxybutyrate-co-3-hydroxyvalerate) (PHBV) has characteristics similar to polypropylene (PP), is non-toxic, compostable and has high crystallinity, which makes it competitive to replace PP and has been applied as food packaging material for example⁴⁻⁶. Compostable polymers can be completely degraded, generating water molecules and carbon oxide as byproducts, making them ideal to avoid polymer waste generation⁷.

In terms of pilot scale production and thermal processability, studies of PHBV indicate its potential for

packaging and foodservice applications due to its good oxygen/water vapor barrier properties, but some drawbacks still greatly limit its processing and application, such as inherent brittleness, physical aging at room temperature and narrow processing windows. In addition, its degradation can occur even during storage, further reducing the molar mass and consequently the properties, making commercial use of this polymer difficult. The short processability window and fluid instability are other negative features of the application of this pure polymer, making it difficult to expand its use in packaging^{8,9}, but its excellent gas barrier property makes it attractive in packaging application¹⁰.

The formation of composite material has been pointed out as a possibility for using this polymer, in addition to reducing the amount of polymeric matrix. Natural fibers can be used as reinforcement of biocomposites in the PHBV matrix, producing completely biodegradable composites with a rapidly biodegradable matrix, which increases their applications and attractiveness¹¹⁻¹³. Cellulose is an attractive source of filler, since in addition to being widely used, in the polymer matrix in packaging¹⁴⁻¹⁷. Recycled paper has potential as a source of low-cost cellulose fibers^{18,19}.

In the process of reusing cellulose fibers, reversible and irreversible chemical and physical changes occur. These changes are inherent to the fibers themselves, and can include loss of swelling capacity and reduction of moisture, these being especially important in packaging applications.

*e-mail: daniele.bastos@uerj.br

Paper is a resource with high abundance of cellulose fiber, in particular, China produces hundreds of millions of tons of waste paper every year, which can be used with great economic benefit^{20,21}.

The aim of this work was to produce fully biodegradable rigid packaging using a compostable polymeric matrix with short fiber cellulose residues.

2. Experimental Procedures

2.1. Materials

PHBV powder with 4 wt.% of HV was supplied by PHB Industrial S.A. (São Paulo, Brazil). The number (Mn) and weight (Mw) average molar mass, and polydispersion index ($I=Mw/Mn$) were measured by gel permeation chromatography (GPC) with a Shimadzu LC Solution chromatograph using a chloroform column. For this, 6.0 mg of powdered PHBV was evaluated with an injected volume of approximately 2 μ L. The evaluation of molar mass by GPC indicated Mn and Mw values of 80.10^3 and $170.10^3 \text{ g}\cdot\text{mol}^{-1}$, respectively. Cellulose paper (sulphite A4 sheet of paper) after use was reused by passing through a simple fiber separation step. The shredded paper was placed in a beaker with water and after soaking for 30 minutes it was submitted to agitation with an IKA RW 20 digital propeller agitator for 30 minutes at 30 rpm until the fibers were separated in solution. Then the fibers were dried in an oven for 40 minutes at 80 °C.

2.2. Preparation of composites

A pre-mixing step of the PHBV and Cellulose (CE), PHBV/CE composite, was performed employing two systems. First, a Marconi MA500 mill with sintered ceramic balls was used, and a second attempt was made by replacing the ceramic balls with metal rollers. The other premixing method was applied using an Ika A11 analytical mill for 30 s, this was adopted as the method of premixing the composite. Compositions with 0, 5, 10, 15 and 20% by mass of cellulose were obtained to produce formulations with PHBV/CE proportions of 100/00, 95/05, 90/10, 85/15 and 80/20. Each formulation was extruded in a twin-screw extruder (TeckTril DCT model) equipped with 10 temperature zones, ranging from 190 to 110 °C from the feed to die, and rotating at 43 rpm. The test specimens for characterization were obtained by pressing the bulk samples from the extrusion at a temperature of 200 °C for 300 s, with pressure of 5 tons, followed by cooling in a cold press for 200 s.

2.3. Characterization

2.3.1. Scanning electron microscopy (SEM)

A FEI Quanta 400 scanning electron microscope equipped with energy dispersive spectroscopy (EDS) with a Bruker-AXS Quantax detector, acceleration voltage of 20 kV and a working distance of 11 mm was employed to analyze samples coated with gold.

2.3.2. Fourier-transform infrared spectroscopy (FTIR)

The composition of the samples of PHBV/CE was evaluated using Fourier-transform infrared spectroscopy (FTIR) with a Nicolet 6000 model from Thermo Fisher Scientific equipped with an attenuated total reflectance (ATR) accessory.

The analysis was performed in the region of 4000–650 cm^{-1} , with 64 scans.

2.3.3. Thermogravimetric analysis (TGA)

The thermal stability and mass loss of the PHBV/CE composites were evaluated by thermogravimetric analysis using a PerkinElmer Pyris 1 analyzer with a heating range of 25 °C to 500 °C and a heating rate of 10 °C/min under N_2 atmosphere with a flow rate of 60 mL/min.

2.3.4. Differential scanning calorimetry (DSC)

The thermal behavior of the PHBV/CE composites with different mass ratios was evaluated by differential scanning calorimetry (DSC) with a Hitachi DSC 7020 thermal analysis system using heating and cooling rates of 10 °C/min and nitrogen atmosphere flow (50 mL/min). Two heating and one cooling cycle were carried out. The first heating cycle was conducted from 0 to 200 °C, followed by cooling to –20 °C and subsequent heating from –20 °C to 200 °C. The first heating run was used to erase the thermal history of the samples, while their thermal parameters were obtained from the second heating run. The crystallinity degree of the samples was calculated by the following Equation 1:

$$X_c(\%) = \Delta H_f(1-W) / (\Delta H_f^0 \cdot 100) \quad (1)$$

Where ΔH_f^0 is the enthalpy of crystalline PHBV 100% ($146.6 \text{ J}\cdot\text{g}^{-1}$)²², ΔH_f is the enthalpy of the sample, and W is the cellulose fiber (CE) fraction present in the sample.

2.3.5. Contact angle

Two methods were used to measure the contact angle: the force-based method (or Wilhelmy method) and the sessile drop method using a Ramé-Hart NRL A 100-00 goniometer, measuring speed at 3 mm/min. For the force-based method, the advancing contact angle was measured by obtaining the perimeter of rectangular samples, which were then placed in a tensiometer (Kruss K100K) along with the surface tension of the liquid (water) to determine the wettability. The sessile drop method involved depositing a 2 μ L drop of distilled water onto the surface of each sample at room temperature, and measuring the contact angles in triplicate.

2.3.6. X-ray diffraction (XRD)

The XRD analysis was performed with a Bruker-AXS D8 Advance Eco diffractometer, using Cu $\text{K}\alpha$ radiation ($\lambda = 1.54180 \text{ \AA}$, 40 kV/25 mA) and 2θ angle range from 4° to 70°.

2.3.7. Impact resistance

The impact tests were carried out in accordance with ASTM D256²³ with an impact pendulum (CEAST 9050), with a 2.7 J impact hammer.

2.3.8. Vicat softening temperature

The test was performed according to ASTM D-1525²⁴, with a CEAST HV3 6911.000 tester. At least three Vicat softening temperature test repetitions were conducted for each formulation and the averages were calculated. The test parameters were imposed stress of 50 N and initial temperature of 25 °C.

2.3.9. ANOVA

To verify the effect of adding of cellulose waste (CE) on the PHBV, an analysis of variance (ANOVA) Post hoc Test–Fisher’s Least Significant difference (LSD) was performed adopting a 0.05 significance level ($p < 0.05$)²⁵.

3. Results and Discussion

Figure 1, shows the SEM images of the cellulose fibers from recycled paper (Figure 1a) and the cross-section surface of the PHBV/CE composites obtained by varying the concentration of cellulose fibers, Figure 1b-f.

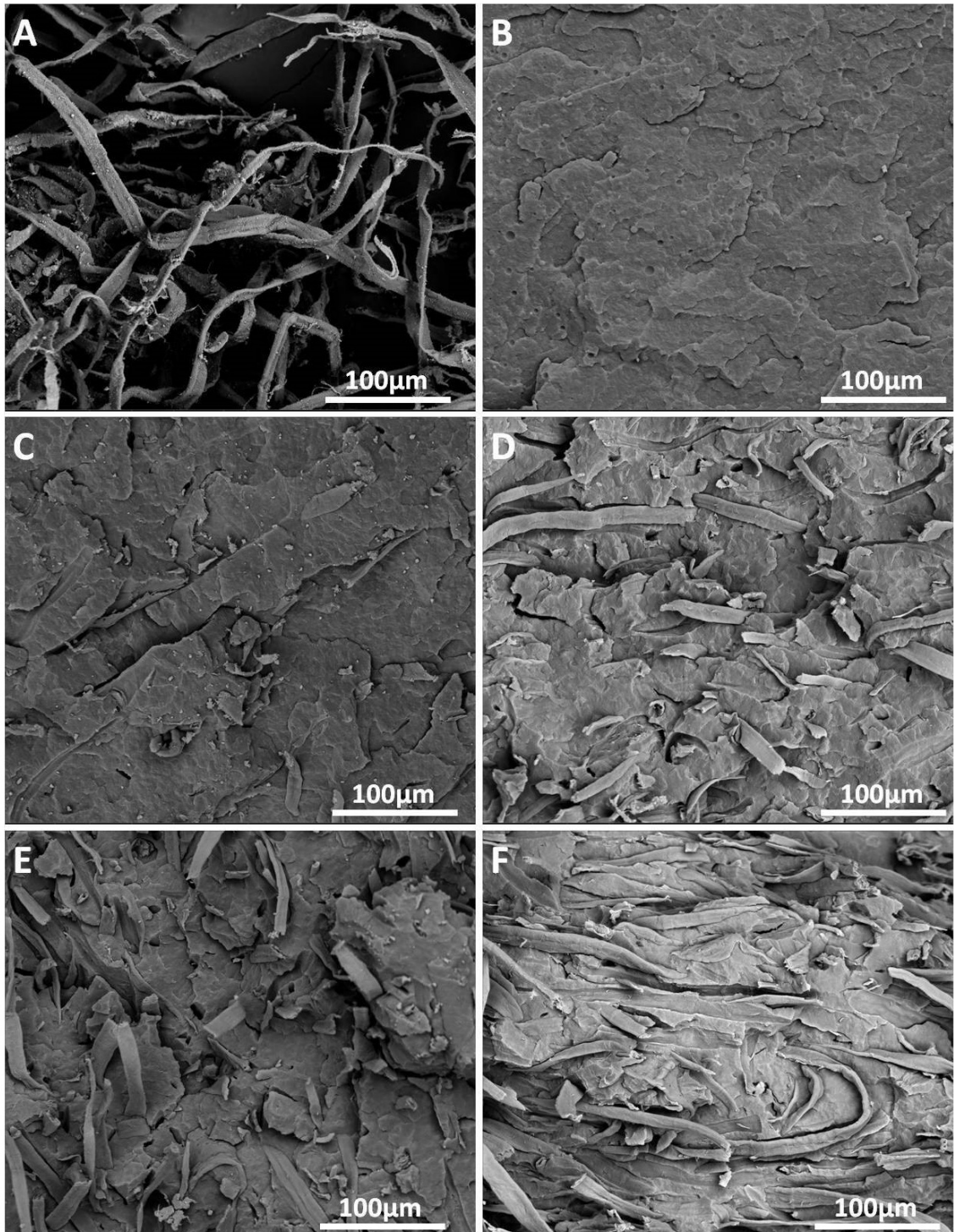


Figure 1. SEM micrographs of cellulose and formulations: A) CE; B) 100-00; C) 95-05; D) 90-10; E) 85-15; F) 80-20.

The increase in the polymer/filler mass ratio (PHBV/CE) generated larger defects on the composite surface, such as a rougher surface as a function of rising CE concentration, revealing the incorporation of cellulose fibers in the polymeric matrix. Morphologies characteristic for this filler as reported in the literature^{26,27}.

The FTIR spectra obtained for PHBV, cellulose fibers and composites in the wavenumber regions between 4000 cm^{-1} and 750 cm^{-1} and between 1500 cm^{-1} and 600 cm^{-1} are shown in Figures 2 and 3 respectively. Peaks near 2975 and 2745 cm^{-1} (C-H groups) were observed. A strong and sharp band at 1724 cm^{-1} , characteristic of the axial deformation of the ester group (C=O), of PHBV was observed. The band at 1380 cm^{-1} corresponds to the asymmetric deformation of the C-H bond of the methyl group. The characteristic band of symmetrical and asymmetrical stretching of the C-O-C group is present at 1132 cm^{-1} .

The bands representing the axial deformation of the C-O and C-C bonds are present at 1275, 1052 cm^{-1} and 979 cm^{-1} respectively (Figure 3), whereas this broadening and increased intensity in the bands allocated at 1050 cm^{-1} may suggest some interaction and presence of cellulose in the PHBV/CE composite^{28,29}. Studies of PHBV loaded with performed by Yu et al.³⁰, Yu and Qin³¹ and Ponjavic et al.³², presented similar spectra to that observed by us.

Figure 4a and b and Table 1 shows the thermal transitions and crystallization behavior of neat PHBV and PHBV/CE composites during the first and the second heating runs of DSC assay. The first heating destroyed the entire crystalline structure, so the thermal history of the samples was eliminated. In the second heating, the increase in cellulose content (5 to 20 wt%) promoted a slight reduction in the melting point of PHBV (T_{m2}) compared with the neat PHBV (169.4 °C) showed in Table 1. Also, the incorporation of cellulose may favor the formation of a small population of more imperfect crystals which are consistent with previous reports in the literature³³. This imperfect crystals, melt at a lower temperature ($\sim 150^\circ\text{C}$) as observed in Figure 4b. The addition of cellulose (5 to 15 wt%) improved the crystallization degree of PHBV in approximately 15 wt%, for these formulations. However, the increase in cellulose content for 20 wt% showed a similar value for the neat PHBV (~ 42 wt%).

Figure 4c and d and Table 2 shows the TGA results of PHBV, cellulose fibers and composites. The cellulose had lower thermal stability than neat PHBV and its composites, considering the T_{onset} values. The cellulose fibers presented two thermal events related to mass loss. At a temperature of 41 °C there was mass loss, which corresponds to the release of volatiles, mainly absorbed water.

The second mass loss process started at a temperature of 293 °C, with maximum degradation temperature of 349 °C, ending at 394 °C. According to Cordeiro et al.³⁴, this temperature range may be related to the thermal degradation of fiber components lignocellulosic substances, mainly cellulose, which occurs at 340 °C. For PHBV, the mass loss was gradual and uniform with increasing temperature.

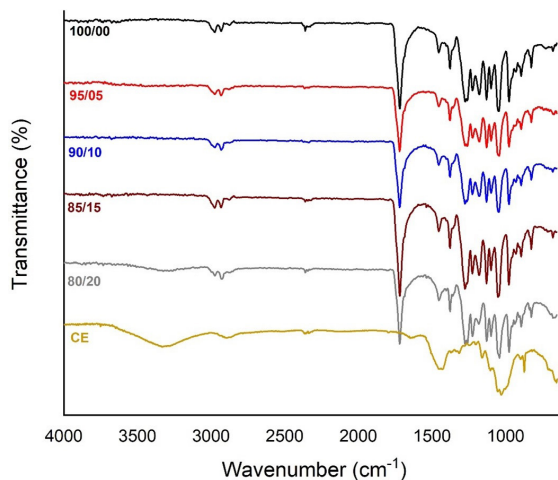


Figure 2. FTIR-ATR spectra of cellulose fibers and formulations (4000 cm^{-1} and 750 cm^{-1}).

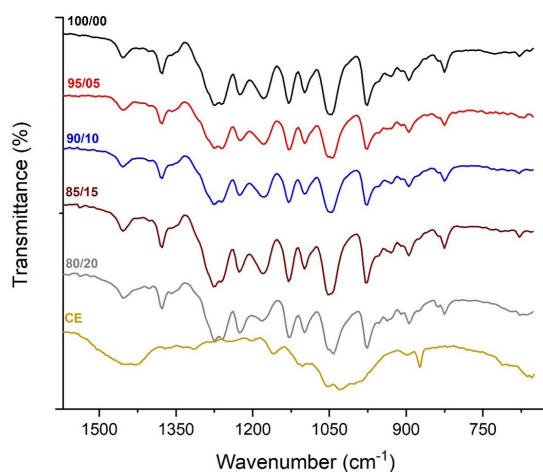


Figure 3. FTIR-ATR spectra of cellulose fibers and formulations (1500 cm^{-1} and 6000 cm^{-1}).

Table 1. DSC results – Thermal transitions of the second heating cycle for formulations.

Sample	T_{m1} (°C)	T_{m2} (°C)	ΔH_m (J.g ⁻¹)	X_c (%)
100/00	-	169.4	62.4	42.6
95/05	150.6	167.9	79.0	56.7
90/10	151.5	166.1	75.5	57.2
85/15	151.7	165.9	69.1	55.5
80/20	150.4	163.5	49.0	41.8

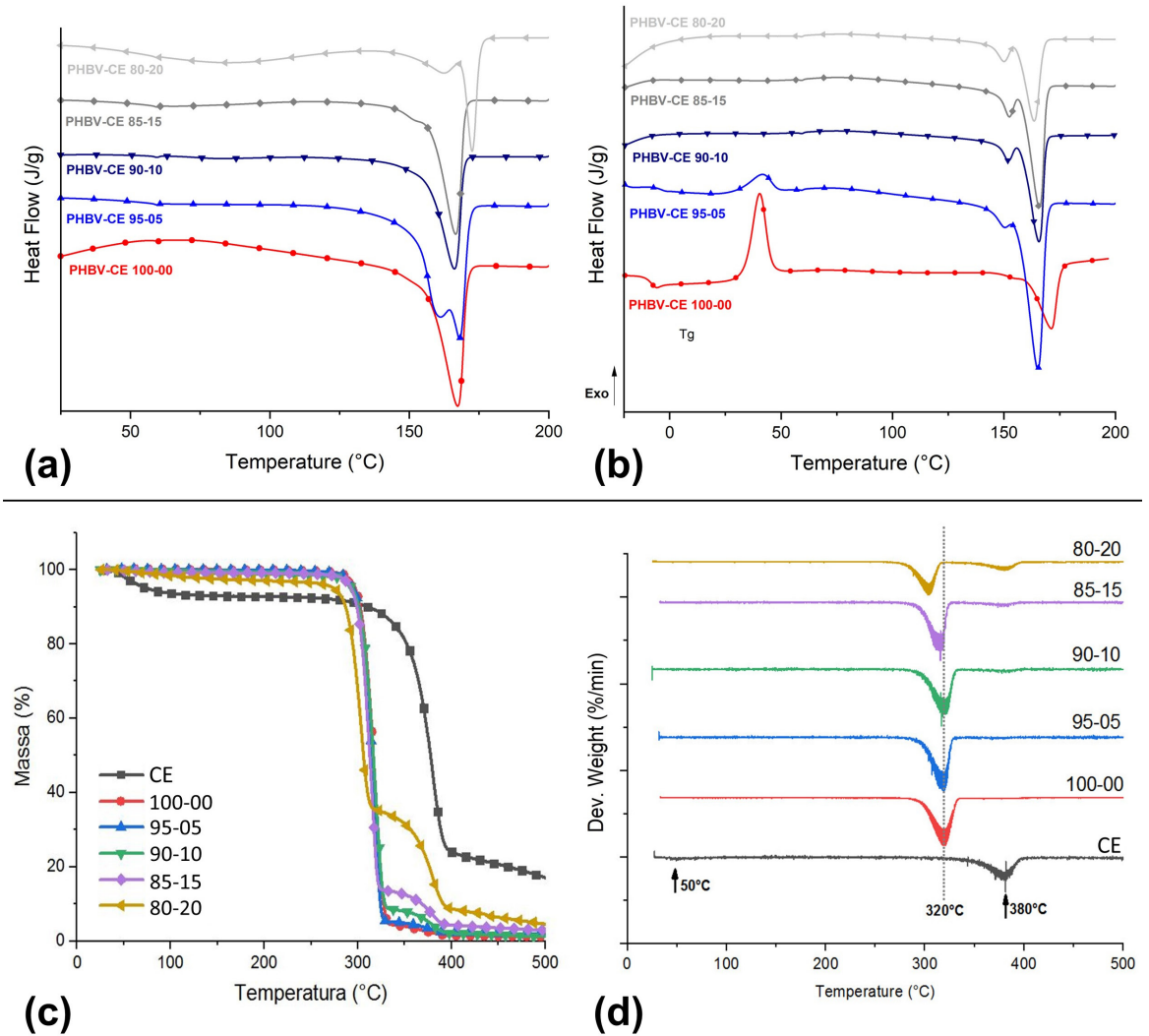


Figure 4. Thermal behavior from cellulose fiber and formulations: DSC curves for samples with different relation PHBV/CE. (a) First heat cycle and (b) Second heat cycle; TG (c) and DTG (d) curves.

Table 2. Thermal characteristics (TGA) of cellulose (CE), PHBV and PHBV/CE composites.

	Degradation event	T _{onset} (°C)	T _{max} (°C)	T _{endset} (°C)	Mass loss (%)
CE	1°	41	57	79	93
	2°	293	349	394	24
100/00	1°	276	294	332	4
	2°	354	362	388	1
95/05	1°	270	293	326	5
	2°	369	375	388	2
90/10	1°	269	293	330	9
	2°	356	367	391	2
85/15	1°	271	291	322	13
	2°	349	361	389	4
80/20	1°	258	281	310	36
	2°	342	361	390	8

The thermal degradation of PHBV occurred in two stages of mass loss. The first mass loss process started at a temperature at 276 °C and ended close to 332 °C, with maximum degradation temperature of 294 °C. The second mass loss process started at 354 °C, with maximum degradation temperature of 362 °C, ending at 388 °C. This temperature is almost 26 and 104 °C, respectively, higher than that reported in literature ($T_{\text{onset}} = 250$ °C)³⁵.

With respect to the first degradation event of the PHBV/CE composites, the increase in cellulose content (5 to 15 wt%) did not change the thermal stability of the polymer. The TGA curves of the composites showed practically the same thermal degradation behavior, with mass variation onset temperature around 270 °C and maximum degradation temperature around 293 °C. The PHBV/CE composites with the highest cellulose content (20 wt%) were less thermally stable. The increase in the cellulose percentage caused the approximation of molecular chains, leading to the formation of agglomerates³⁶. Similar results were observed by Bhardwaj et al.³⁷, who reported that the TGA curves of PHBV composites undergo thermal degradation above 250 °C and that T_{onset} of thermal degradation of the PHBV composites is like that of pure PHBV except for the composite with higher cellulose content. Considering the second degradation event, all materials showed similar behavior, with reduced thermal stability compared to pure PHBV. Different amounts of residues were formed in the PHBV composites. The amount of residue was higher in composites with a higher amount of cellulose fibers.

Figure 5 shows the XRD results. The XRD of PHBV showed two main diffraction peaks, which are typical of a structure of PHB in $2\theta \approx 13.4^\circ$ and 16.8° relative to crystallographic planes (020) and (110). The other peaks in 2θ near to 20.0° ; 21.4° ; 22.5° ; 25.4° and 27.1° , are related to crystallographic planes (021), (100), (101), (111), (130) and (040). Studies of PHBV performed by Macedo et al.³⁸, and Wang et al.³⁹, presented diffraction peaks like that observed by us. Cellulose diffractograms showed typical behavior of semicrystalline structures. Two well-defined peaks referring to the amorphous and crystalline phases are visualized. The lowest intensity peak refers to the amorphous phase and is close to $2\theta = 17^\circ$, whereas the most intense peak is related to the crystalline portion and is close to $2\theta = 21^\circ$ ^{40,41}. The increase in the cellulose content (5 to 20% in weight) promoted a small decrease in the intensity of crystalline phases referring to the plane of PHBV in the composites as the load concentration increased. The composite with the lowest cellulose content (95/5) showed a variation in the peaks close to $2\theta = 22^\circ$, suggesting a variation in the crystalline structure of the PHBV polymeric matrix.

Roughness and porosity are features that make the analysis of contact angle of cellulose samples difficult^{42,43}. Therefore, performing contact angle measurements by tensiometry on porous materials was indicated as a good alternative⁴⁴. Figure 6 displays the force-tensiometry curve profile as a function of sample displacement, highlighting that the curve of pure PHBV and the sample containing 5% cellulose exhibited similar behavior, whereas the remaining compositions displayed similarity differently. Similarly, such behavior was observed by Szymczyk and Podkościelna⁴⁵ in a cellulose composite.

The dynamic contact angle results measured by using force tensiometry and drop method can be seen in Table 3. The contact angle of 78° of the pure polymer sample indicated its hydrophilic character, but the insertion of cellulose promoted characteristics of hydrophobicity, as indicated by the increase in the angle to 100.52° . As indicated by the micrographs, the insertion of the cellulose promoted an increase in surface roughness, drastically altering the surface characteristics, which was determinant in the wettability of the composites⁴⁶.

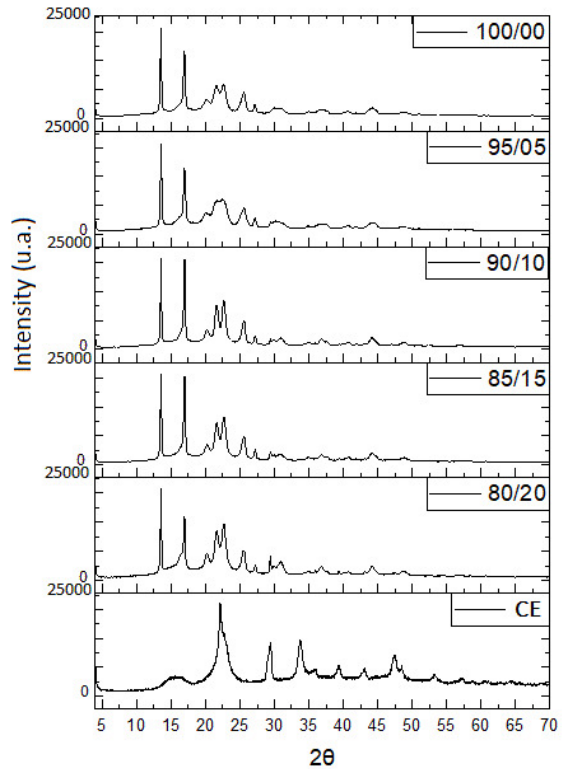


Figure 5. Diffractogram of the formulations.

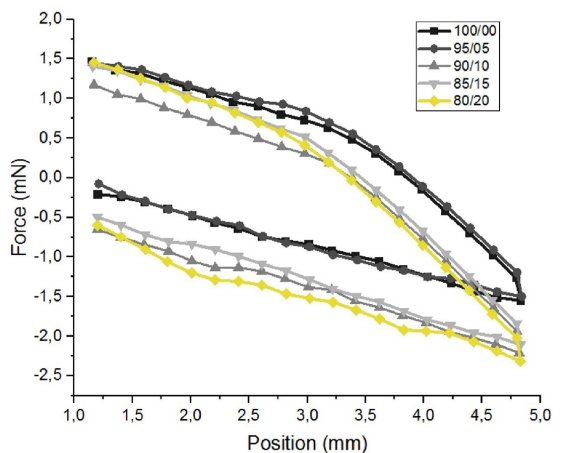


Figure 6. Contact angle measurements using the Wilhelmy method.

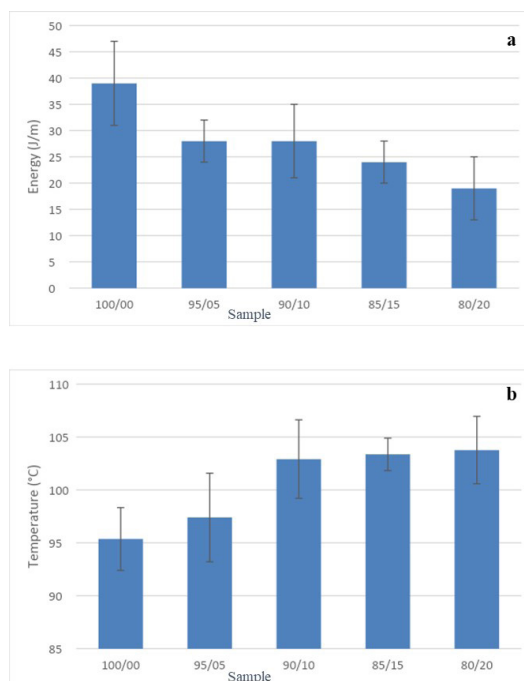
Table 3. Contact angle results of formulations by Drop and Wilhelmy method:

Sample	Drop method (°)	Wilhelmy method (°)
100/00	77.7 ± 2,0	78.01
95/05	90.0 ± 3,8	82.72
90/10	82.1 ± 3,7	87.66
85/15	83.3 ± 0,2	88.77
80/20	76.0 ± 0,7	100.52

Similarly, according to the drop method, the increase in cellulose content indicated a trend towards increased hydrophobicity of the material, with values ranging from 77.7 ± 2.0 for pure PHBV to 90.0 ± 3.8 for the composition with 5% cellulose.

Figure 7a shows the impact resistance results of the PHBV and composites. The PHBV sample had higher impact resistance. For PHBV/CE composites, the increase in cellulose content (5 to 20 wt%) reduced the impact resistance. For PHBV composites containing 20% cellulose, the impact strength reduced by 40% compared with the neat PHBV. This decrease occurred because the addition of cellulose causes a decrease in the mobility of the polymeric chains, reducing the capacity of the composite to absorb energy. This decrease in impact resistance may be a consequence of cellulose agglomerations in the composites, acting as stress concentration points, from which cracks propagate. Similar results were observed by Ahankari et al.⁴⁷ who reported that the addition of lignocellulosic fibers to the PHBV matrix promoted reduction impact strength of composites. According to the authors, this was due to the formation of fiber agglomerates in the matrix, increasing the stresses and making the material more brittle, and consequently reducing the energy needed to break the samples. On the other hand, the impact resistance shown significance variation for samples with major amount of filler (CE). Samples 80/20 and 85/15 presented $LSD > 0.0168$, referring statistically significance compared with neat PHBV (100/00) sample. However, for the samples with minor amount of CE, the variation of impact resistance was minor significant, this significance was calculated by Analyze of Variance (ANOVA) post Hoc Test – Fisher's Least Significant Difference (LSD) (calculated $LSD = 0.995$).

The thermal resistance of the neat PHBV and PHBV/CE composites was evaluated by measuring the Vicat softening temperature (VST). Figure 7b shows the relationship between Vicat and the incorporated cellulose content in the composite. The PHBV showed Vicat temperature of 95 °C, while the composite with 5% CE showed Vicat of 98°C and the composites with 10, 15 and 20% presented Vicat softening temperature close to 103 °C, increases of 3% and 8%, respectively, in relation to the Vicat temperature of the neat polymer. The increase in Vicat results from the restriction of the mobility of the polymeric chains in the presence of the cellulose, increasing the dimensional stability of the PHBV, so higher temperatures are necessary to reach a given deformation level, increasing the dimensional stability of the polymeric matrix⁴⁸. The increase in Vicat softening point caused by the presence of cellulose is an important technological contribution to the production of composites, since one of the limitations of PHBV for technological applications is its short processability.

**Figure 7.** Results of impact resistance (a) and Vicat softening temperature (b) of PHBV/CE formulations ($p < 0.05$).

Therefore, the composites can be used in environments with higher temperatures than possible with PHBV alone while maintaining the dimensional stability.

ANOVA - (LSD) (calculated $LSD = 0.869$) for Vicat softening temperature indicates that increasing levels of cellulose fibers as the filler on PHBV matrix were statistically significant between 100/00 and major amount of CE 90/10, 85/15, 80/20 samples ($LSD > 0.0168$). On the other hand, the increase of cellulose for minor relation (95/05) shows not influential on the impact resistance ($LSD < 0.883$) demonstrating that with 5 wt. % of CC don't has influence in the variation on softening temperature.

4. Conclusions

An analytical mill was used to promote the dispersion of cellulose fibers making PHBV powder and cellulose fibers more dispersed and homogeneous. In the SEM images, it was possible to observe the increase of irregularity of the material surface due to the increase of roughness that was a dominant effect of the increase of the contact angle. The FTIR analysis suggested that the cellulose fibers acted as nucleating agents based on the lower intensity of the peaks in the regions of 980 and 1230 cm^{-1} . The TGA results indicated two thermal events concerning the polymer and cellulose where the composite samples presented close T_{onset} values, except for the 80/20 composition, which started degrading at lower temperature. The DSC results indicated increased crystallinity of the polymer, in agreement with the FTIR results. The XRD peaks of the pure cellulose were less intense in relation to the polymer matrix, so the cellulose peaks were not prominent in the composite samples. In particular in sample 95/05 a change in the curve profile was noticeable.

The increase in the amount of cellulose caused a reduction in the mobility of the molecules. In addition to the increase of crystallinity, there was a reduction in impact strength as well as an increase in the formation of agglomerates, which acted as stress concentrators. Finally, the Vicat softening temperature increased with increase of cellulose, which is very positive for PHBV, which has a short processability window.

5. Acknowledgments

We thank FAPERJ and CNPq for financial support. Multi-user laboratory of materials characterization COPPE/UFRJ and multi-user of microscopy of CETEM.

6. References

- Chia RW, Lee JY, Jang J, Cha J. Errors and recommended practices that should be identified to reduce suspected concentrations of microplastics in soil and groundwater: a review. *Environmental Technology & Innovation*. 2022;28:102933.
- Roy T, Dey TK, Jamal M. Microplastic/nanoplastic toxicity in plants: an imminent concern. *Environ Monit Assess*. 2023;195:27.
- Manu MK, Luo L, Kumar R, Johnravindar D, Li D, Varjani S, et al. A review on mechanistic understanding of microplastic pollution on the performance of anaerobic digestion. *Environ Pollut*. 2023;325:121426.
- Dedieu I, Aouf C, Gaucel S, Peyron S. Mechanical recyclability of biodegradable polymers used for food packaging: case study of polyhydroxybutyrate-co-valerate (PHBV) plastic. *Food Addit Contamin Part A*. 2022;39(1):1878-92.
- Figuerola-Lopez KJ, Prieto C, Pardo-Figueroa M, Cabedo L, Lagaron JM. Development and characterization of electrospun poly(3-hydroxybutyrate-co-3-hydroxyvalerate) biopapers containing cerium oxide nanoparticles for active food packaging applications. *Nanomaterials (Basel)*. 2023;13:823.
- Bonnenfant C, Gontard N, Aouf C. PHBV-based polymers as food packaging: physical-chemical and structural stability under reuse conditions. *Polymer (Guildf)*. 2023;270:125784.
- Varghese SA, Pulikkalparambil H, Rangappa M, Siengchin S, Parameswaranpillai J. Novel biodegradable polymer films based on poly(3-hydroxybutyrate-co-3-hydroxyvalerate) and Ceiba pentandra natural fibers for packing applications. *Food Packag Shelf Life*. 2020;25:100538.
- Wu F, Misra M, Mohanty AK. Challenges and new opportunities on barrier performance of biodegradable polymers for sustainable packaging. *Prog Polym Sci*. 2021;117:101395.
- Carlos ALM, Mancipe JMA, Dias ML, Thiré RMSM. Poly(3-hydroxybutyrate-co-3-hydroxyvalerate) core-shell spun fibers produced by solution blow spinning for bioactive agent's encapsulation. *J Appl Polym Sci*. 2022;139(18):52081.
- Wu F, Feng D, Xie YH, Xie D, Mei Y. Role of phase compatibility in gas barrier improvement of biodegradable polymer blends for food packaging application. *Ind Eng Chem Res*. 2022;61:5464-74.
- Lammi S, Gastaldi E, Gaubiac F, Angellier-Coussy H. How olive pomace can be valorized as fillers to tune the biodegradation of PHBV based composites. *Polym Degrad Stabil*. 2019;166:325-33.
- Alane A, Zembouai I, Benhamida A, Zaidi L, Touati N, Kaci M. *Opuntia ficus indica* fibers as reinforcement in PHBV biocomposites. *Mater Today Proc*. 2022;53:218-22.
- Mazur KE, Jakubowska P, Gawel PA, Kuciel S. Mechanical, thermal and hydrodegradation behavior of poly(3-hydroxybutyrate-co-3-hydroxyvalerate) (PHBV) composites with agricultural fibers as reinforcing fillers. *Sustain Mater Technol*. 2022;31:e00390.
- Halloub A, Raji M, Essabir H, Chakchak H, Boussem R, Bensalah M, et al. Intelligent food packaging film containing lignin and cellulose nanocrystals for shelf life extension of food. *Carbohydr Polym*. 2022;296:119972.
- Xu K, Li Q, Xie L, Shi Z, Su G, Harper D, et al. Novel flexible, strong, thermal-stable, and high-barrier switchgrass-based lignin-containing cellulose nanofibrils/chitosan biocomposites for food packaging. *Ind Crops Prod*. 2022;179:114661.
- Yang W, Fortunati E, Dominici F, Giovanale G, Mazzaglia A, Balestra GM, et al. Synergic effect of cellulose and lignin nanostructures in PLA based systems for food antibacterial packaging. *Eur Polym J*. 2016;79:1-12.
- Qazanfarzadeh Z, Ganesan AR, Mariniello L, Conterno L, Kumaravel V. Valorization of brewer's spent grain for sustainable food packaging. *J Clean Prod*. 2023;385:135726.
- Huang D, Hong H, Huang W, Zhang H, Hong X. Scalable preparation of cellulose nanofibers from office waste paper by an environment-friendly method. *Polymers (Basel)*. 2021;13:3119.
- Oliveira DM, de Bomfim ASC, Benini KCCC, Cioffi MOH, Voorwald HJC, Rodrigue D. Waste paper as a valuable resource: an overview of recent trends in the polymeric composites field. *Polymers (Basel)*. 2023;15(2):426.
- Yoshida A. China's ban of imported recyclable waste and its impact on the waste plastic recycling industry in China and Taiwan. *J Mater Cycles Waste Manag*. 2022;24:73-82.
- Jiang Q, Xing X, Yi J, Han Y. Preparation of cellulose nanocrystals based on waste paper via different systems. *Int J Biol Macromol*. 2020;149:1318-22.
- Ting ZX, Yan LJ. Effects of bacterial cellulose whisker melting composite on crystallization and mechanical properties of PHBV composites. *Macromol Res*. 2022;30:325-33.
- ASTM: American Society For Testing Materials. ASTM D256-10: standart test methods for determining the Izod pendulum impact resistance of plastics. West Conshohocken, PA: ASTM; 2018.
- ASTM: American Society For Testing Materials. ASTM D1525-17: standart test methods for vicat softening temperature of plastics. West Conshohocken, PA: ASTM; 2007.
- Rabello LG, Ribeiro RCC. Bio-based polyurethane resin: an ecological binder for a novel class of building materials-composites. *Mater Lett*. 2022;311:131566.
- Li A, Xu D, Li Y, Wu S, Madyan OA, Rao J, et al. Binary additives of polyamide epichlorohydrin-nanocellulose for effective valorization of used paper. *Int J Biol Macromol*. 2023;226:194-201.
- Soto M, Rojas C, Cárdenas-Ramírez JP. Characterization of a thermal insulating material based on a wheat straw and recycled cellulose to be applied in buildings by blowing method. *Sustainability*. 2023;15:58.
- Bai J, Dai J, Li G. Electrospun composites of PHBV/pearl powder for bone repairing. *Prog Nat Sci*. 2015;25(4):327-33.
- Abbasi M, Pokhrel D, Coats ER, Guho NM, McDonald AG. Effect of 3-hydroxyvalerate content on thermal, mechanical, and rheological properties of poly(3-hydroxybutyrate-co-3-hydroxyvalerate) biopolymers produced from fermented dairy manure. *Polymers (Basel)*. 2022;14:4140.
- Yu HY, Qin ZY, Sun B, Yang XG, Yao JM. Reinforcement of transparent poly(3-hydroxybutyrate-co-3-hydroxyvalerate) by incorporation of functionalized carbon nanotubes as a novel bionanocomposite for food packaging. *Compos Sci Technol*. 2014;94:96-104.
- Yu HY, Qin ZY. Surface grafting of cellulose nanocrystals with poly(3-hydroxybutyrate-co-3-hydroxyvalerate). *Carbohydr Polym*. 2014;101:471-8.
- Ponjavic M, Malagurski I, Lazic J, Jeremic S, Pavlovic V, Prlainovic N, et al. Advancing PHBV biomedical potential with the incorporation of bacterial biopigment prodigiosin. *Int J Mol Sci*. 2023;24(3):1906.

33. Benini KCCC, Cioffi MOH, Voorwald HJC. PHBV/cellulose nanofibrils composites obtained by solution casting and electrospinning process. *Materia (Rio J)*. 2017;22(2):e-11837.
34. Cordeiro EMS, Nunes YL, Mattos ALA, Rosa MF, Souza MSM Fo, Ito EN. Polymer biocomposites and nanobiocomposites obtained from mango seeds. *Macromol Symp*. 2014;344:39-54.
35. Dasan YK, Bhat AH, Ahmad F. Polymer blend of PLA/PHBV based bionanocomposites reinforced with nanocrystalline cellulose for potential application as packaging material. *Carbohydr Polym*. 2017;157:1323-32.
36. Singh S, Mohanty AK. Wood fiber reinforced bacterial bioplastic composites: fabrication and performance evaluation. *Compos Sci Technol*. 2007;67:1753-63.
37. Bhardwaj R, Mohanty AKM, Drzal LT, Pourboghrat F, Misra M. Renewable resource-based green composites from recycled cellulose fiber and poly(3-hydroxybutyrate-co-3-hydroxyvalerate) bioplastic. *Biomacromolecules*. 2006;7(6):2044-51.
38. Macedo JS, Costa MF, Tavares MIB, Thiré RMSM. Preparation and characterization of composites based on polyhydroxybutyrate and waste powder from coconut fibers processing. *Polym Eng Sci*. 2010;50:1466-75.
39. Wang C, Hsu C, Hwang I. Scaling laws and internal structure for characterizing electrospun poly [(R) -3-hydroxybutyrate] fibers. *Polymer (Guildf)*. 2008;49:4188-95.
40. Cardoso PHM, Bastian FL, Thiré RMSM. Curaua fibers/epoxy laminates with improved mechanical properties: effects of fiber treatment conditions. *Macromol Symp*. 2014;344:63-70.
41. Oudiani AE, Chaabouni Y, Msahli S. Crystal transition from cellulose I to cellulose II in NaOH treated agave America L. fibre. *Carbohydr Polym*. 2011;86:1221-9.
42. El Omari H, Ablouh EH, Brouillette F, Taourirte M, Belfkira A. New method for determining paper surface energy per contact angle. *Cellulose*. 2019;26:9295-309.
43. Krainer S, Hirn U. Contact angle measurement on porous substrates: effect of liquid absorption and drop size. *Colloids Surf A Physicochem Eng Asp*. 2021;619:12650.
44. Peršin Z, Stana-Kleinschek K, Sfiligoj-Smole M, Kre T, Ribitsch V. Determining the surface free energy of cellulose materials with the powder contact angle method. *Text Res J*. 2004;74(1):55-62.
45. Szymczyk K, Podkościelna B. Synthesis and wettability of cellulose based composites by aqueous solutions of nonionic surfactant. *Colloids Surf A Physicochem Eng Asp*. 2021;623:126709.
46. Anaya-Mancipe JM, Pereira LCB, Borchio PGM, Dias ML, Thiré RMSM. Novel polycaprolactone (PCL)-type I collagen core-shell electrospun nanofibers for wound healing applications. *J Biomed Mater Res B Appl Biomater*. 2023;111(2):366-81.
47. Ahankari SS, Mohanty AK, Misra M. Mechanical behaviour of agro-residue reinforced poly(3-hydroxybutyrate-co-3-hydroxyvalerate), (PHBV) green composites: a comparison with traditional polypropylene composites. *Compos Sci Technol*. 2011;71:653-7.
48. Santos EF, Moresco M, Rosa SML, Nachtigall SMB. Extrusão de compósitos de PP com fibras curtas de coco: efeito da temperatura e agentes de acoplamento. *Polímeros*. 2010;20(3):215-20.